Modelling of the impurity-vacancy interaction in magnesium doped lithium oxide

1993 J. Phys.: Condens. Matter 5 7397

(http://iopscience.iop.org/0953-8984/5/40/014)

J. Phys.: Condens. Matter 5 (1993) 7397–7408. Printed in the UK

Modelling of the impurity–vacancy interaction in magnesium doped lithium oxide

J L Gavartin†‡, A L Shluger†‡ and C R A Catlow‡

† Department of Chemical Physics of Condensed Matter, University of Latvia, 19 Rainis Boulevard, Riga, Latvia

‡ The Royal Institution of Great Britain, 21 Albemarle Street, London W1X 4BS, UK

Received 26 May 1993, in final form 22 July 1993

Abstract. The influence of the Mg^{2+} impurity on cation migration in Li_2O crystals is considered. A static atomistic simulation technique is used to study the most stable forms of impurity–vacancy association. The adiabatic barriers for the vacancy motion in the presence of Mg^{2+} impurity ions in Li_2O are calculated and discussed. The formation of impurity–vacancy $(Mg^{2+}–V_c)_n$ clusters and their possible further association is investigated.

1. Introduction

Crystalline Li_2O is of considerable technological and fundamental interest both as a 'blanket' material for deuterium–tritium fusion reactions and as a 'fast ionic conductor'. It has the anti-fluorite structure with the Li^+ ions forming a simple cubic sublattice and O^{2-} ions in the centres of alternate cubes. It is natural to suggest that in Li_2O there are converse mechanisms for the conductivity to those for fluorite structured materials [1, 2]: the ionic current should be due to the *cation* diffusion through the lattice by vacancy nearest-neighbour (NN) hops and by interstitial jumps (with an interstitialcy mechanism). Both experimental data [3–6] and computer modeling studies [1–3, 7, 8] indeed suggest that cation diffusion is predominant in Li_2O just as anion transport dominates in fluorite structured solids.

As with other ionic conductors, the ionic transport is affected by doping. The Li_2O crystal may be doped to appreciable concentrations by Mg^{2+} or F^- impurities, due to the high solubility of MgO and LiF within the Li_2O lattice, which in turn rests on the similarity in the ionic size of Li^+ and Mg^{2+} ions. The impurity Mg^{2+} ion substitutes for the host cation in the Li_2O matrix, and the corresponding cation vacancy is created by charge compensation.

There have been relatively few studies of the role of Mg dopant in Li_2O. Chadwick and co-authors [3, 4] calculated the thermodynamic parameters for cation–Frenkel defect formation and migration in Li_2O and the cation conductivity plot which they compared with those observed experimentally for pure and Mg doped crystals. The agreement between the results of the simulations and the experimental data for doped samples was unsatisfactory. They suggested that the shifted intrinsic region of the measured ionic conductivity of the doped samples could result from a strong Mg–cation vacancy association. Jacobs and Vernon [7] calculated the association energies of the Mg–vacancy NN and NNN complexes and found them to be very similar. Since both impurities and vacancies may be mobile at high temperatures the effects of dipole clustering are likely to occur.

Clustering and aggregation are very common phenomena in ionic solid solutions. The most widely studied systems are the rare earth doped alkaline earth fluorides [2, 9–11], and

0953-8984/93/407397+12$07.50

alkaline earth doped alkali halides [12–21], in which the influence of clustering on both ionic and electronic properties was found to be very significant. It was shown that the size and structure of impurity–vacancy associates depend on the ionic size of the dopant relative to that of the host ion.

The dipolar association and clustering has been studied extensively in LiF:Mg [13–18], which has similarities to Mg doped Li_2O. In LiF, the Mg^{2+} ion also substitutes for the Li^+ ion but within the face centred cubic (FCC) lattice, and creates a corresponding cation vacancy. Taylor and Lilley [17] demonstrated that the distribution of the impurity–vacancy dipoles in this system at a given temperature depends strongly on the thermal prehistory of the sample. It was suggested that the dipoles cluster mainly into trimers [17–20]. However, formation of the so-called Suzuki phase was also found to be possible [21].

The purpose of the present paper is to consider the influence of the Mg^{2+} impurity in Li_2O in more detail. In particular, we used a static atomistic simulation technique to study the most stable forms of impurity–vacancy association. The results of our calculations of the adiabatic barriers for the ionic motion in the presence of Mg^{2+} impurity ions in Li_2O are presented and discussed. The formation of impurity–vacancy $(Mg^{2+}–V_c)_n$ clusters and their possible further association is investigated.

In the next section we give a short description of the method of calculation and the potentials used. An approximate estimation of vacancy motion in the presence of an Mg^{2+} ion and the results of more detailed atomistic simulation of impurity–vacancy dipole formation are presented in section 3. The possible mechanisms of dipole diffusion are discussed in section 4, and the results of simulations of $(Mg^{2+}–V_c)_n$ aggregates ($n = 1$–8) are reported in section 5. The electronic structure of the most stable $(Mg^{2+}–V_c)_4$ cluster is discussed in section 5.1. The final discussion and conclusions are given in section 6.

2. Calculation procedure

Our simulations have used the MOLSTAT code [22], which is based on the pair potential method [23], and is analogous to the well known HADES code for studying defects in ionic crystals. The differences between MOLSTAT and HADES were described earlier [8], but they are insignificant in our studies. Both codes allow one to calculate the energy of the defect in the crystal by minimizing the energy with respect to displacements of the surrounding atoms. The interatomic potentials include Coulomb and short-range terms, while the shell model is used to include ionic polarization effects. Short-range interactions are assumed to be pairwise and are described using a Buckingham form:

$$V(r) = A\exp(-r/\rho) - C/r^6 \tag{1}$$

where the first term represents the Pauli repulsion between electron shells, and the second term models dispersion and covalent interaction effects. In the present work we employed the same pair potentials for Li_2O:Mg which were used previously by Chadwick and co-authors (CFSH) [3]. The parameters for Li_2O were empirically fitted in order to reproduce the crystal structure, the phonon spectra and the elastic and dielectric constants of the pure Li_2O crystal [24]. The general features of the ionic model employed in atomistic simulations have been discussed in detail in previous publications (see for example reviews by Stoneham and Harding [25], Harding [26] and Catlow and Stoneham [23]). However, as we shall see later, the formation of large clusters of impurity–vacancy dipoles is accompanied by a dramatic change in the coordination number of O^{2-} ions within the cluster. As was demonstrated in [27] this can lead to an electron density redistribution between ions.

To investigate this latter point we performed quantum chemical calculations for the most stable impurity–vacancy cluster using the CLUSTER code [28]. The method employed in this code allows us to find the electronic structure of perfect and defective crystals within the embedded cluster [29] or supercell model [30]. The intermediate neglect of differential overlap (INDO) approximation is used in order to solve the Hartree–Fock–Roothaan equations [31]. This method uses semiempirical parameters for the calculation of some of the elements of the Fock matrix. These parameters were fitted to reproduce the electronic structure and lattice constant of the perfect Li_2O and MgO crystals and the related diatomics [32]. The advantages of using quantum chemical and molecular simulations in a consistent way are discussed elsewhere [16].

3. Simulation of the Mg^{2+}–V_c interaction

Diffusion of the vacancy can be sensibly described as a drift in a periodic crystalline potential E_f perturbed by the presence of the impurity ion. The influence of an Mg^{2+} ion in its simplest form can be modelled by including a screened Coulomb term:

$$E_c = -1/\varepsilon r \tag{2}$$

where r (in atomic units) is the Mg^{2+}–V_c separation, and ε is the dielectric constant of the Li_2O crystal. We can investigate the extent to which this simple model is correct by performing detailed calculations of the interactions of vacancies with Mg^{2+} impurities. In particular, we explore the energetics of vacancy jumps around the Mg^{2+} ion dopant. In doing this we assume that Mg^{2+} ions occupy only lattice sites (we neglect the possibility of their interstitial location).

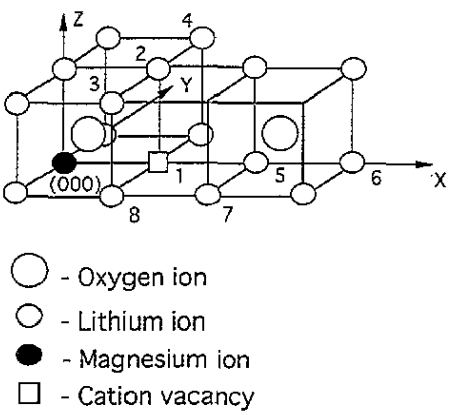

Figure 1. Impurity–vacancy configurations examined *in the calculations. Numbers (1–8) denote different* vacancy positions relative to the impurity ion.

Geometric configurations of the cation vacancy in the vicinity of the Mg^{2+} ion considered in our study are presented schematically in figure 1. The calculated static energies of these configurations and adiabatic barriers for the vacancy jumps are summarized in tables 1 and 2. The defect association energy is defined as

$$\Delta U_0 = E_{Mg-V_c} - E_{Mg} - E_{V_c} \tag{3}$$

Table 1. The calculated energies (in eV) for different configurations of Mg^{2+}–V_c dipoles (figure 1). In calculating the association energies $-\Delta U_0$ as defined by equation (3) the following quantities were used: $E_{Mg} = -13.32$ eV and $E_{V_c} = 5.05$ eV. For the continuum approximation energy $-E_c$: $\epsilon = 10$ and $a_0 = 4.36$ a.u.

V_c location	Defect energy	ΔU_0	E_c
1: (100)	−8.83	−0.56	−0.62
2: (101)	−8.58	−0.31	−0.44
3: (1−11)	−8.49	−0.22	−0.36
4: (111)	−8.53	−0.26	−0.36
5: (200)	−8.63	−0.36	−0.31
6: (300)	−8.51	−0.24	−0.21
7: (2−10)	−8.46	−0.19	−0.18
∞	−8.27	0.00	0.00

Table 2. The adiabatic barriers (in eV) for different V_c jumps towards and away from Mg^{2+} ion (see figure 1).

Jump direction	Towards barrier	Away from barrier
4–2	0.15	0.20
3–2	0.17	0.26
2–1	0.08	0.33
6–5	0.05	0.21
5–1	0.03	0.23
7–5	0.12	0.29
7–8	0.13	0.25

where E_{Mg} is the defect energy of the isolated Mg^{2+} ion at the cation site, E_{V_c} denotes the formation energy of the cation vacancy, and E_{Mg-V_c} is the defect energy of the Mg^{2+}–V_c pair in the configuration examined.

From the comparison made in table 1 one can see that for a separation of more than $2a_0$ (a_0 is the cation–cation distance) the association energies of the impurity–vacancy dipole become similar to those obtained from the screened Coulomb attraction in the quasi-continuum model described above. The elastic interaction between the defects is relatively small and even at small impurity–vacancy separations the effects of the Coulomb attraction predominate. As one can see from table 2, the activation energies for the vacancy hops towards the Mg^{2+} ion are generally smaller than those for the jumps in the opposite direction. They clearly depend on the trajectory by which the vacancy approaches the impurity ion. Inspection of table 2 suggests that if a cation vacancy finds itself inside a sphere with a centre on the Mg^{2+} ion and with a radius of about $3a_0$, it will be trapped by the impurity with a large probability in the NN position (position 1 in figure 1). The most probable trajectory for this process is along the ⟨100⟩ axis (positions 6–5–1 in figure 1). The dissociation energy of the corresponding final ⟨100⟩ dipole is 0.56 eV.

4. Impurity–vacancy dipolar diffusion

In our previous simulations we assumed that the Mg^{2+} ion was frozen in the cation site, and only the vacancy was allowed to move. However, at high enough temperatures impurity–vacancy dipole diffusion becomes feasible. This problem has been studied extensively in alkali halides during the last two decades using different experimental [12, 17–21] and

theoretical [12–16] techniques. The results suggest that M^{2+}–V_c dipoles can move through the FCC structured lattice without dissociation. The latter might be even more significant for the Mg^{2+}–V_c dipoles in the more compact cation sublattice of Li_2O. In this section we shall discuss the results of modelling possible mechanisms of the impurity–vacancy dipole diffusion through the anti-fluorite structured lattice of Li_2O.

Let us first consider the migration of the Mg^{2+} ion by the vacancy mechanism. The calculated adiabatic barrier for the Mg^{2+} jump into the NN (100) vacant position is 1.28 eV. That for the jump into the NNN (110) vacant position is found to be 2.15 eV. Since the barrier for the V_c (100) jump was found to be only 0.19 eV [8], we conclude that the Mg^{2+} ion is significantly less mobile than the host Li^+ ion. This is due to the interaction of the impurity excess charge with the crystalline field in the initial state, and the repulsion of the nearest cations in the transition state. Therefore we can suggest that migration of a single dipole consists of two steps: a 90° reorientation of the dipole, and an Mg^{2+} ion jump (see figure 2). The reorientation can occur in at least three different ways: (i) two sequential vacancy jumps from the (100) to the (110) position and then from the (110) to the (010) position (figure 2(*a*)); (ii) the cooperative jump of two Li^+ ions depicted in figure 2(*b*); (iii) the single direct NNN vacancy jump from the (100) to the (010) position (figure 2(*c*)).

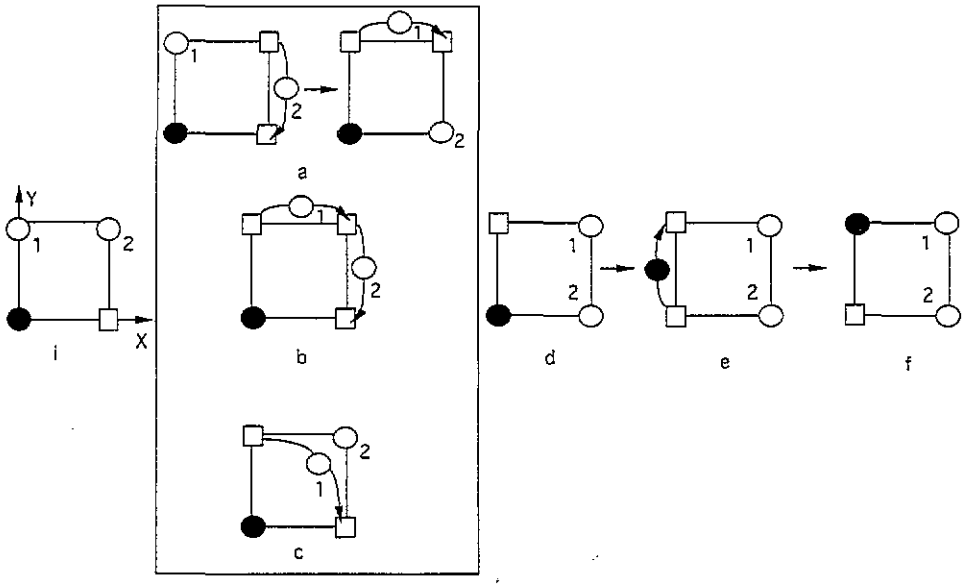

Figure 2. Schematic representation of the mechanisms for the Mg^{2+}–V_c dipolar diffusion within the (100) cation plane: i, the initial configuration; a, b, c, the three possible mechanisms for 90° reorientation of the dipole, resulting in configuration d; e, the Mg^{2+} ion's jump; f, the final configuration. (For notation see figure 1.)

The barrier for the first mechanism of reorientation (figure 2(*a*)) is controlled by the first vacancy hop—away from the Mg^{2+} ion because of the smaller barrier for the reverse jump—and is calculated to be 0.33 eV. The barriers calculated for the mechanisms (ii) and (iii) are considerably larger: 1.1 and 1.62 eV, respectively. Therefore one can conclude that Mg^{2+}–V_c dipole diffusion should be dominated by the first mechanism and is controlled by the Mg^{2+} jumps, which have a barrier substantially higher than that for rotation of the impurity–vacancy dipole.

One can also consider different more complex mechanisms for dipole diffusion, which can involve, for instance, the association of an additional cation vacancy with the Mg^{2+}–V_c dipole and the subsequent motion of a V_c–Mg^{2+}–V_c trimer. The barrier energy for the jump of the Mg^{2+} ion might be considerably reduced in this situation. An additional vacancy can be created as a result of a Frenkel Li^+ interstitial–vacancy pair formation either near the dipole, or somewhere far away from that. In the latter case the vacancy can be attracted due to the effective vacancy–dipole interaction. We considered several possible configurations corresponding to the creation of a Frenkel pair close to the dipole. The aim of these calculations was to investigate whether reduction of the barrier for the jump of the Mg^{2+} ion would partly compensate the formation energy of the undissociated Li^+ Frenkel pair. Our calculations demonstrated that this process is energetically much less favourable than the second possibility of trapping by the dipole of a vacancy from a fully dissociated Frenkel pair, which results from the strong repulsion between the Mg^{2+} and the Li^+ interstitial ion. Therefore we consider the V_c–Mg^{2+}–V_c trimer, assuming the charge compensating Li^+ ion to be far from it.

The binding energy ΔU_v of the cation vacancy to the dipole is given by

$$\Delta U_v = E_{V_c\text{–dip}} - E_{Mg-V_c} - E_{V_c}. \tag{4}$$

Here $E_{V_c\text{–dip}}$ is the defect energy of the V_c–Mg^{2+}–V_c associate. In table 3 we compare the ΔU_v values for different compact configurations of the vacancy–dipole associates corresponding to the various vacancy positions near the frozen (100) dipole depicted schematically in figure 3.

Table 3. The calculated energies (in eV) as defined by equation (4) for the different configurations of V_{c1}–Mg^{2+}–V_{c2} associates, when the coordinates of the magnesium ion are a_0(000), and V_{c1} – a_0(100) (see figure 3).

V_{c2} location	Defect energy	ΔU_v
1: (−100)	−4.08	−0.30
2: (−200)	−3.97	−0.19
3: (−110)	−3.94	−0.16
4: (−11−1)	−3.94	−0.16
5: (−300)	−3.88	−0.10
6: (010)	−4.05	−0.27
7: (110)	−3.50	0.28
8: ∞	−3.78	0.00

The binding energy ΔU_v arises from the charge–dipole interaction and the local lattice distortions, which decrease the total energy of the associate. Although, the V_c–Mg^{2+}–V_c trimer has many possible mechanisms for diffusion, it is clear from the simulations that the jump of the Mg^{2+} ion controls the rate of the dipolar diffusion. We have found only one configuration of the V_c–Mg^{2+}–V_c trimer for which the barrier energy for the Mg^{2+} ions' jump (0.8 eV) is less than that for the single dipole. This corresponds to the initial state with location of the second vacancy in site 7 (see figure 3). However, the probability of this mechanism is negligible due to strong repulsion between two vacancies and the instability of the initial configuration (see table 3). Therefore, we conclude that the most efficient mechanism for dipolar diffusion does not involve the creation of an additional vacancy, but presumably concerns the dipolar 90° reorientation discussed earlier in this section.

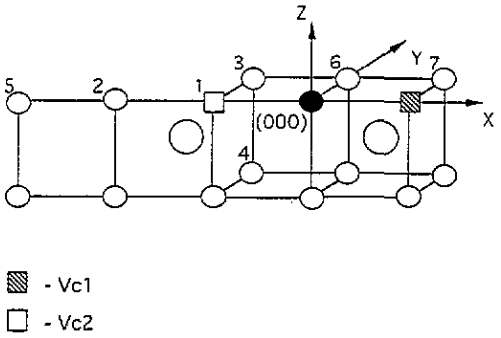

Figure 3. Vacancy–impurity–vacancy configurations considered in calculations. Numbers (1–7) indicate various locations of the second vacancy, V_{c2}, relative to the fixed Mg^{2+}–V_{c1} dipole. Coordinates of the Mg^{2+} ion are $a_0(000)$, and V_{c1} – $a_0(100)$. (For notation see figure 1.)

5. Study of the $(Mg^{2+}–V_c)_n$ clusters

The importance of possible association effects in highly disordered materials has been discussed by several authors (see for example the review in [9]). Detailed discussions have been given of the defects associated with M^{2+} impurities in fluorides [1, 10–11]. In this section we consider the problem of clustering in the cation sublattice of Li_2O in terms of cluster binding energies. We note that although dipoles can dissociate at high temperatures, diffusion of the Mg^{2+} ion occurs by a vacancy mechanism (i.e. a Mg^{2+} ion always needs a vacancy within the first cation sphere for its jump).

It is plausible to suggest that clustering of several vacancies and impurities can be considered as an association of individual dipoles. The related binding energies can be defined as

$$\Delta U_n^{\text{bind}} = E_n/n - E_1 \tag{5}$$

$$\Delta U_n^{\text{assoc}} = E_n - E_{n-1} - E_1 \tag{6}$$

where E_n denotes the defect energy of the cluster of n Mg^{2+}–V_c dipoles. ΔU_n^{bind} is a binding energy of the cluster per component Mg^{2+}–V_c dipole; $\Delta U_n^{\text{assoc}}$ reflects the energy change when a new dipole is associated with the cluster of $n-1$ dipoles. Negative values for these energies mean that the energy of the cluster is lower than that of its isolated constituent species (dipoles, or cluster plus one dipole). We do not take into account the entropy changes that accompany cluster formation, i.e. the contribution of the entropy term to the formation enthalpy is assumed to be small (see [33] and [34] for discussion).

The most stable dipole clusters are shown schematically in figure 4. In considering their relative stability we note first that the Li^+ and Mg^{2+} ions have very similar ionic radii. Therefore the contribution of the electrostatic impurity–lattice interaction to the defect energy is significantly larger than that of the elastic deformation energy of the lattice near the Mg^{2+} ion. In order to restrict the number of configurations that may be produced from several dipoles we assumed that the most stable clusters will have the smallest multipole moment. This conjecture was confirmed by the results of our simulations. The corresponding binding energies are summarized in table 4. We note that dimers *a*, *b* and *c* (figure 4) have no dipole moment, and that the higher stability of dimer *a* is due to the small dipole–dipole separation. The fact that trimer *d* has a larger binding energy per dipole than that of *e* can also be related

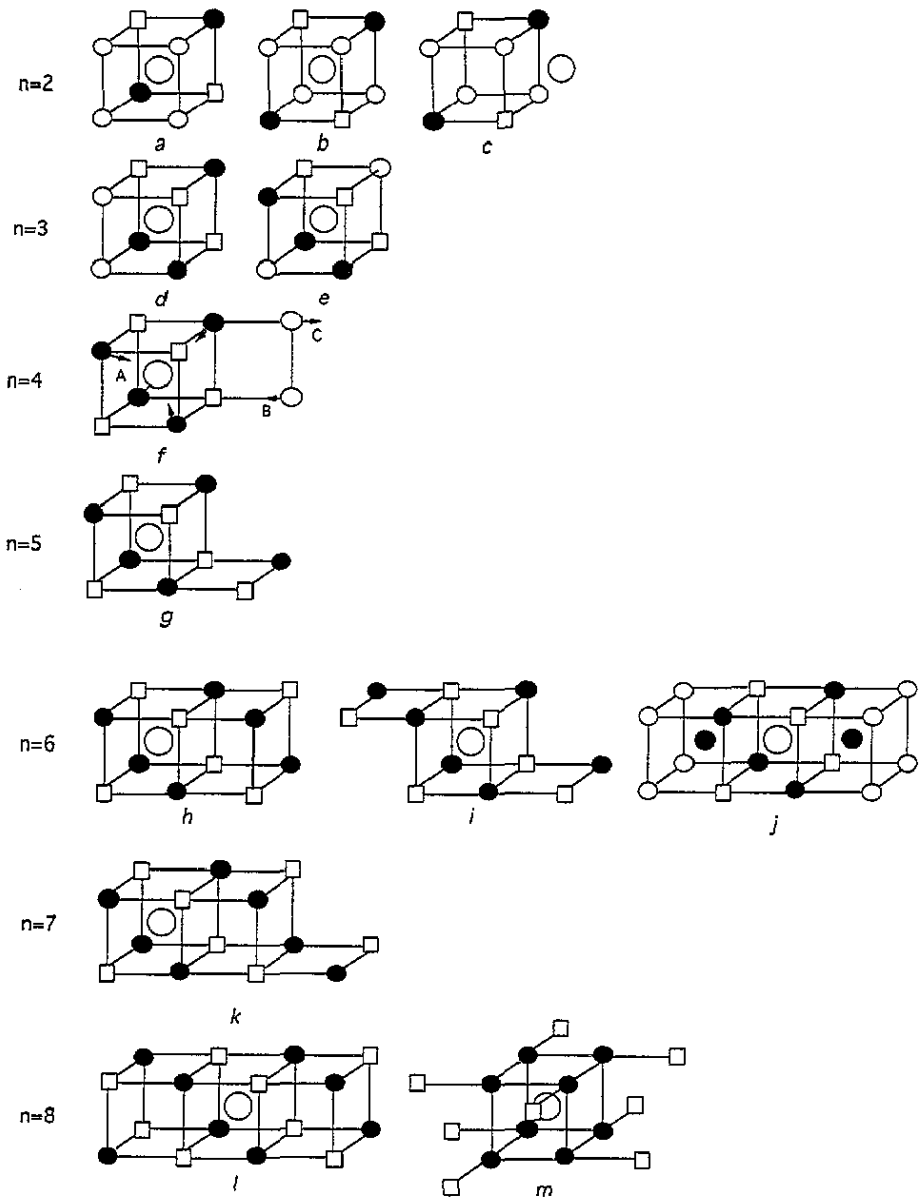

Figure 4. The calculated clusters of the Mg^{2+}–V_c dipoles within the Li_2O lattice. Only vacant lattice sites and Mg^{2+} ions, and several host ions (when necessary), are shown for simplicity. The arrows indicate the directions of displacement of non-equivalent ions for the tetramer (*f*); A corresponds to the displacement of four Mg^{2+} ions; B represents the displacement of 12 Li^+ ions nearest to the vacancy, and C that of 12 Li^+ ions nearest to the Mg^{2+} ions. (For notation see figure 1.)

to its much smaller dipole moment. Our simulations demonstrated that the cluster binding energy increases considerably with the number of dipoles within the range $n = 1$–4; and that tetramer *f* is the most stable small cluster, with a much larger binding energy than any trimer.

Table 4. The calculated defect, binding (ΔU_n^{bind}), and association (ΔU_n^{assoc}) energies as defined by equations (5) and (6) (in eV) of the various $(Mg^{2+}\text{–}V_c)_n$ clusters shown in figure 4. The configurations *a*, *d* and *i* shown in brackets correspond to the $(n-1)$ dipole clusters (see equation (6) and figure 4).

		Defect energy	ΔU_n^{bind}	ΔU_n^{assoc}
$n=2$	*a*	−18.23	−0.28	−0.57
	b	−17.71	−0.02	−0.05
	c	−17.82	−0.08	−0.16
$n=3$	*d*	−27.56	−0.36	−0.50 (*a*)
	e	−27.26	−0.26	−0.20
$n=4$	*f*	−37.53	−0.55	−1.14 (*d*)
$n=5$	*g*	−46.76	−0.52	−0.35
$n=6$	*h*	−55.97	−0.50	−0.38
	i	−56.48	−0.58	−0.89
	j	−55.09	—	—
$n=7$	*k*	−65.70	−0.56	−0.39 (*i*)
$n=8$	*l*	−75.41	−0.60	−0.88
	m	−67.65	—	—

In order to understand whether there is a further increase in the binding energy with an increase of the cluster size we have calculated a few possible larger aggregates containing five to eight dipoles. In particular, we have chosen clusters which could be precursors for the FCC structured (*j*), BCC structured (*m*) and tetrahedral structured phases (*g*, *h*, *i*, *k*, *l*) of MgO within the Li_2O matrix. The calculations demonstrated that formation of FCC like and BCC like clusters of MgO is not energetically favourable at least for small 'crystallites'. Essentially the crystalline field of the anti-fluorite crystal structure of Li_2O forces the clusters of dipoles to aggregate into the sphalerite (ZnS) structure, for which the tetramer (*f*) is a precursor. MgO has a rock salt structure, and in contrast with other alkaline earth oxides, polymorphism of the pure MgO crystal is not observed at least for pressures below 1 Mbar [31]. So, in this case the sphalerite structure is stabilized only by the constraints of the surrounding anti-fluorite lattice. Its influence decreases as the aggregate grows. Although the clusters of five to eight dipoles continue to remain stable (figure 4 and table 4), their association energy ΔU_n^{assoc} is much smaller than that for the tetramer.

It is reasonable to assume that the mobility of any dipolar associate is much smaller than that for a single dipole. In this case the associates are growing only by joining an additional dipole. Considering the equilibrium conditions, we can obtain the relation between the concentrations of various clusters using the mass action law:

$$N_n = N_{n-1} N_1 A_n \exp(H_n/kT). \tag{7}$$

Here the index n denotes the cluster size, N_n is the stationary concentration of the clusters of n dipoles, A_n is a constant which includes the entropy changes associated with clustering reaction, and H_n is the binding enthalpy of the corresponding cluster. For present purposes it is almost certainly acceptable to approximate H_n by ΔU_n^{assoc}. This energy is larger for the tetramer than for any other cluster. Thus tetramers will dominate in some temperature interval. However, the question of the cluster distribution needs more detailed investigation.

The stability of the tetramer f is largely determined by its high symmetry (which coincides with the local symmetry of the crystalline lattice), and the similarity between the Mg–O distance in this cluster and that in the MgO cubic crystal (which are 2.0 and 2.1 Å, respectively). The displacements of the Mg^{2+} ions from the lattice sites are only $0.01\sqrt{3}a_0$ (A in figure 4(f)). However, the surrounding lattice is deformed strongly by the tetramer, and the relaxation of nearest ions is almost $0.09a_0$ for modes B and C (figure 4(f)). At the same time, the relaxation of the NNN O^{2-} ions is about $0.05a_0$.

As we stressed earlier, the model employed assumes a fully ionic approximation. Nevertheless, it is possible that the formation of the tetrahedral structure may lead to an electronic charge redistribution towards greater covalence, which is common for sphalerite structured systems. It was also shown that in small MgO clusters the magnitudes of Mg and O ionic charges increase slowly with the cluster size and remain far below the values expected for the solid state [27, 35]. In the next section we will address this question using a quantum mechanical study of the tetramer.

5.1. The electronic structure of the $(Mg^{2+}–V_c)_4$ cluster

The electronic structure of the $(Mg^{2+}–V_c)_4$ tetramer was calculated using the CLUSTER code and the embedded molecular cluster model. We considered three different clusters: $[(Mg^{2+}–V_c)_4Li_{32}O_{13}]^{6+}$ (PL6), $[(Mg^{2+}–V_c)_4Li_{32}O_{19}]^{6-}$ (M6) and $[(Mg^{2+}–V_c)_4Li_{32}O_{16}]^{0}$ (ZC). These were chosen in order to compare the effects of cluster size. The PL6 cluster consists of the tetramer shown in figure 4(f), which is fully coordinated by the first sphere of 12 O^{2-} ions and the second sphere of 32 Li ions. The M6 cluster has an additional sphere of six O^{2-} ions. The ZC cluster has only three O^{2-} ions in the second anion coordination sphere in order to neutralize the cluster charge. The electronic structure of the perfect Li_2O crystal was calculated using the neutral cluster with the same number of sites as ZC, and the periodic large unit cell model. The results of the calculations, which are qualitatively the same for all three clusters, can be summarized as follows.

(i) The results of Löwdin population analysis show that the ionic charges within the tetramer are very similar to those in the perfect lattice ($Q_{Li} \simeq 0.87$, $Q_O \simeq -1.8$, and $Q_{Mg} \simeq 1.75$ in units of the electron charge). The central O^{2-} ion, which is fully coordinated by the four Mg^{2+} ions, has the same charge as that for O^{2-} ions of Li_2O.

(ii) The displacements of the four Mg^{2+} ions (mode A in figure 4(f)) are identical to those obtained from the atomistic simulation. However, the values of the displacements of Li^+ ions corresponding to the modes B and C obtained within the two techniques, although qualitatively similar, could not be compared directly due to significant boundary effects in the embedded cluster model.

(iii) The upper valence band of the crystal is determined by the p-type atomic orbitals (AOs) of the O^{2-} ions and has the same width as that obtained for the ideal crystal. The AOs of the central O^{2-} ion do not create local electronic states (contrary to what one might expect). The conduction band is determined by the s-type orbitals of the Li ions. The calculated forbidden gap between the highest occupied and lowest unoccupied state of the perfect crystal is 12.8 eV, which is reasonably close to the experimentally observed optical gap. At the same time the s-type AOs of the magnesium ions produce a set of unoccupied electronic states within the forbidden gap of the crystal at 8.4 eV above the top of the valence band. This value is similar to the optical gap of the MgO crystal.

Similar lattice relaxation determined by both techniques suggests that a difference in charge distribution does not strongly affect the atomic structure. These results support the applicability of the ionic approximation, as is commonly the case for cubic structured ionic compounds [8, 16].

6. Discussion

It is interesting to compare the behaviour of the alkaline earth impurity–vacancy dipoles in alkali oxide and alkali halide crystals. In particular, as was shown in the previous studies [13–15], there is a possibility of both NN and NNN dipoles being present in appreciable concentrations in alkaline earth ion doped alkali halide crystals. The binding energy of the NN complex increases with the dopant radius, while in the case of the NNN complexes the effect is smaller and reversed. Thus the relative energies of NN and NNN dipoles are determined by elastic rather than Coulomb interaction, as reflected in the migration energies between these sites.

Our simulations show rather different behaviour in Mg doped Li_2O. The activation energy for the free vacancy hops is relatively low, and the Coulomb attraction of the impurity makes it even lower (for jumps towards the impurity). Thus in contrast with the alkali halide crystals, the binding energy of the NN complex is determined mainly by the Coulomb attraction between the impurity and vacancy.

This conclusion differs from the results of calculations by Jacobs and Vernon (JV) [7]. They had suggested the association energies of the (100) and (110) impurity–vacancy dipoles to be −0.942 and −0.943 eV respectively (compare with results presented in table 1). Apparently, this is an effect of the short-range parameters used in the calculations. In particular, the parameters fitted by JV predict the value of 8.06 for the static dielectric constant, while with the CFSH parameters we obtained a value of 10. The experimental value of the static dielectric constant is still uncertain [36, 37].

However, we believe that this difference will not affect our main conclusion regarding the stability of the tetramer. This is the most stable small cluster of Mg^{2+}–V_c dipoles in the Li_2O lattice. Its structure is determined by the symmetry of the host lattice and the crystalline field. Further experimental and theoretical studies are needed in order to validate the role of this cluster in dipole aggregation processes at different temperatures.

Acknowledgments

JLG is grateful to the Royal Society for financial support. ALS acknowledges the Canon Foundation in Europe, the Royal Institution of Great Britain and the Royal Society for financial support. The authors are grateful to P W M Jacobs for valuable discussions.

References

[1] Catlow C R A, Norgett M J and Ross T A 1977 *J. Phys. C: Solid State Phys.* **10** 1627
[2] Catlow C R A 1989 *Superionic Solids and Solid Electrolites* (New York: Academic) p 339
[3] Chadwick A V, Flack K W, Strange J H and Harding J 1988 *Solid State Ionics* **28–30** 185
[4] Chadwick A V, Flack K W, Rageb S M, Strange J H and Xie Z H 1992 *Proc. Int. Conf. on Defects in Insulating materials (ICDIM'92) (Nordkirchen)* p 255
[5] Chadwick A V 1991 *Phil. Mag.* A **64** 983; 1990 *J. Chem. Soc. Faraday Trans.* **86** 1157
[6] Strange J H, Rageb S M, Chadwick A V, Flack K W and Harding J H 1990 *J. Chem. Soc. Faraday Trans.* II **86** 1233, 1239
[7] Jacobs P W M and Vernon M L 1990 *J. Chem. Soc. Faraday Trans. II* **86** 1233
[8] Gavartin J L, Catlow C R A, Shluger A L, Varaksin A N, Kolmogorov Yu N 1992 *Modelling Simul. Mater. Sci. Eng.* **1** 29
[9] Catlow C R A 1991 *Phil. Mag.* A **64** 1911
[10] Catlow C R A, Chadwick A V, Greaves G N and Moroney L M 1984 *Nature* **312** 601

[11] Catlow C R A, Chadwick A V, Corish J, Moroney L M and O'Reilly A N 1989 *Phys. Rev.* B **39** 1897
[12] Benci S, Chiari A and Fermi F 1989 *J. Phys.: Condens. Matter* **1** 227, 2945
[13] Bannon N M, Corish J and Jacobs P W M 1985 *Phil. Mag.* **51** 797
[14] Catlow C R A, Corish J, Quigley J M and Jacobs P W M 1980 *J. Phys. Chem. Solids* **41** 231
[15] Jacobs P W M 1989 *J. Chem. Soc. Faraday Trans.* II **85** 415
[16] Gavartin J L, Shidlovskaya E K, Shluger A L and Varaksin A N 1991 *J. Phys.: Condens. Matter* **3** 2237
[17] Taylor G C and Lilley E 1982 *J. Phys. D: Appl. Phys.* **15** 1243, 1253
Taylor G C, Strutt J E and Lilley E 1981 *Phys. Status Solidi* a **67** 263
[18] McKeever S W S and Lilley E 1982 *J. Phys. Chem. Solids* **43** 885
[19] Yuan X L and McKeever S W S 1988 *Phys. Status Solidi* a **108** 545
[20] McKeever S W S 1984 *J. Appl. Phys.* **56** 2883
[21] Bradbury M H and Lilley E 1977 *J. Phys. D: Appl. Phys.* **10** 1261, 1267
[22] Kolmogorov Yu N and Varaksin A N 1991 *Zh. Struct. Chim.* **32** 162
[23] This technique was reviewed in a special issue of *J. Chem. Soc. Faraday Trans.*: Catlow C R A and Stoneham A M (ed) 1989 *J. Chem. Soc. Faraday Trans.* II **85**
[24] Farley T W D, Hayes W, Hull S, Ward R, Hutchings M T and Alba M 1988 *Solid State Ionics* **28–30** 189
[25] Stoneham A M and Harding J H 1986 *Ann. Rev. Phys. Chem.* **37** 53
[26] Harding J 1989 *Ionic Solids at High Temperatures* ed A M Stoneham (Singapore: World Scientific)
[27] Shluger A L, Gale J D and Catlow C R A 1992 *J. Phys. Chem.* **96** 10389
[28] Shluger A L 1985 *Theor. Chim. Acta* **66** 3575
[29] Kantorovich L N 1983 *Phys. Status Solidi* b **120** 77; 1984 *Phys. Status Solidi* b **123** 325; 1986 *Phys. Status Solidi* b **137** 229
[30] Evarestov R A 1982 *Quantum-Chemical Methods in Solid State Theory* (Leningrad: Leningrad University Press)
[31] Pople J A and Beveridge D L 1970 *Approximate Molecular Orbital Theory* (New York: McGraw-Hill)
[32] Stefanovich E, Shidlovskaya E, Shluger A and Zakharov M 1990 *Phys. Status Solidi* b **160** 529
[33] Harding J H 1989 *J. Chem. Soc., Faraday Trans.* II **85** 351
[34] Harding J H 1985 *Phys. Rev.* B **32** 6861
[35] Ziemann P J and Castelman A W 1991 *J. Chem. Phys.* **94** 718
[36] Osaka T and Shindo I 1984 *Solid State Commun.* **51** 421
[37] Flack K W 1992 *PhD Thesis* University of Kent